NRC Publications Archive
Archives des publications du CNRC

Low-temperature noninjection approach to homogeneously-alloyed PbSexS1−x colloidal nanocrystals for photovoltaic applications
Yu, Kui; Ouyang, Jianying; Zhang, Yanguang; Tung, Hsien-Tse; Lin, Shuqiong; Nagelkerke, Robbert A. L.; Kingston, David; Wu, Xiaohua; Leek, Donald M.; Wilkinson, Diana; Li, Chunsheng; Chen, In-Gann; Tao, Ye

National Research Council Canada   Conseil national de recherches Canada

Canada

Low-Temperature Noninjection Approach to Homogeneously-Alloyed PbSe$_x$S$_{1-x}$ Colloidal Nanocrystals for Photovoltaic Applications

Kui Yu,*[†] Jianying Ouyang,[†] Yanguang Zhang,[‡] Hsien-Tse Tung,[†,⊥] Shuqiong Lin,[†] Robbert A. L. Nagelkerke,[†] David Kingston,[§] Xiaohua Wu,[‡] Donald M. Leek,[†] Diana Wilkinson,[∥] Chunsheng Li,[#] In-Gann Chen,[⊥] and Ye Tao[‡]

[†]Steacie Institute for Molecular Sciences, National Research Council of Canada, Ottawa, Ontario, K1A 0R6, Canada

[‡]Institute for Microstructural Sciences, National Research Council of Canada, Ottawa, Ontario, K1A 0R6, Canada

[§]Institute for Chemical Process and Environmental Technology, National Research Council of Canada, Ottawa, Ontario K1A 0R6, Canada

[⊥]Department of Materials Science and Engineering, National Cheng Kung University, 1 Ta-Hsueh Road, Tainan 701, Taiwan
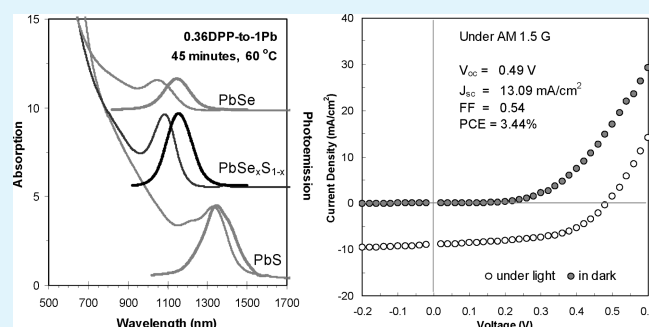
[∥]Defence Research and Development Canada, 3701 Carling Avenue, Ottawa, Ontario, K1A 0Z4, Canada

[#]Healthy Environment and Consumer Safety Branch, Health Canada, Ottawa, Ontario, K1A 1C1, Canada

S *Supporting Information*

ABSTRACT: Homogeneously alloyed PbSe$_x$S$_{1-x}$ nanocrystals (NCs) with their excitonic absorption peaks in wavelength shorter than 1200 nm were developed for photovoltaic (PV) applications. Schottky-type solar cells fabricated with our PbSe$_{0.3}$S$_{0.7}$ NCs as their active materials reached a high power conversion efficiency (PCE) of 3.44%, with an open circuit voltage (V_{oc}) of 0.49 V, short circuit photocurrent (J_{sc}) of 13.09 mA/cm^2, and fill factor (FF) of 0.54 under Air Mass 1.5 global (AM 1.5G) irradiation of 100 mW/cm^2. The syntheses of the small-sized colloidal PbSe$_x$S$_{1-x}$ NCs were carried out at low temperature (60 °C) with long growth periods (such as 45 min) via a one-pot noninjection-based approach in 1-octade-

cene (ODE), featuring high reaction yield, high product quality, and high synthetic reproducibility. This low-temperature approach employed Pb(oleate)$_2$ as a Pb precursor and air-stable low-cost thioacetamide (TAA) as a S source instead of air-sensitive high-cost bis(trimethylsilyl)sulfide (($TMS)_2$S), with n-tributylphosphine selenide (TBPSe) as a Se precursor instead of n-trioctylphosphine selenide (TOPSe). The reactivity difference of TOPSe made from commercial TOP 90% and TBPSe made from commercial TBP 97% and TBP 99% was addressed with in situ observation of the temporal evolution of NC absorption and with ^{31}P nuclear magnetic resonance (NMR). Furthermore, the addition of a strong reducing/nucleation agent diphenylphosphine (DPP) promoted the reactivity of the Pb precursor through the formation of a Pb–P complex, which is much more reactive than Pb(oleate)$_2$. Thus, the reactivity of TBPSe was increased more than that of TAA. The larger the DPP-to-Pb feed molar ratio, the more the Pb–P complex, the higher the Se amount in the resulting homogeneously alloyed PbSe$_x$S$_{1-x}$ NCs. Therefore, the use of DPP allowed reactivity match of the Se and S precursors and led to sizable nucleation at low temperature so that long growth periods became feasible. The present study brings insight into the formation mechanism of monomers, nucleation/growth of colloidal composition-tunable NCs, and materials design and synthesis for next-generation low-cost and high-efficiency solar cells.

KEYWORDS: DBPSe/TBPSe, thioacetamide (TAA), reducing agent, diphenylphosphine (DPP), homogeneously alloyed PbSe$_x$S$_{1-x}$ nanocrystals, quantum dots, photovoltaics

■ INTRODUCTION

Colloidal semiconductor nanocrystals (NCs) such as lead-based quantum dots (QDs) have generated intense interest as important active materials in various applications including photovoltaic (PV) devices.[1−4] Schottky-type solar cells based on PbSe or PbS binary nanocrystals have been explored. For the

PbSe and PbS NCs with similar bandgap, it was documented that PbSe-based Schottky-type solar cells usually exhibited relatively

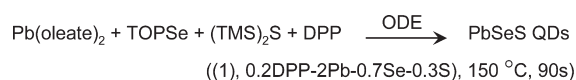large short circuit photocurrent (J_{sc}), while PbS-based cells are distinguished by relatively large open circuit voltage (V_{oc}).[1] Both PbSe and PbS QDs exhibit strong size-dependent properties because of strong quantum confinement, with large exciton Bohr radii of 46 nm for PbSe and 20 nm for PbS and small bandgap of 0.28 eV or 4.43 μm for bulk PbSe and 0.41 eV or 3.03 μm for bulk PbS.[5,6] Meanwhile, PbSe and PbS QDs show simple electron spectra with both charge carriers (with enhanced confinement) contributing almost equally to their exciton Bohr radii; thus, the confinement energy splits approximately equally between the electron and hole carriers.[6]
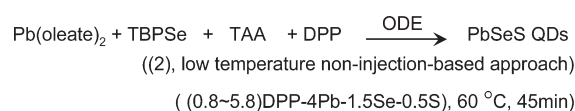
Good performance of homogeneously alloyed $PbSe_{0.3}S_{0.7}$ NC-based Schottky-type solar cells was reported by Ma and co-workers and argued to be related to a combination of the PbSe and PbS properties together with a redistribution of the trap states.[3] The $PbSe_{0.3}S_{0.7}$ NCs were synthesized via a hot-injection approach in 1-octadecene (ODE) at 150 °C, as shown by equation 1. A mixture of n-trioctylphosphine selenide (TOPSe), bis(trimethylsilyl) sulfide ((TMS)$_2$S), and diphenylphosphine (DPP) was rapidly injected into a Pb precursor Pb(oleate)$_2$ solution at 150 °C, with fixed 0.1DPP-to-1Pb and 2Pb-to-1(Se + S) feed molar ratios. It was argued that TOPSe was less reactive than (TMS)$_2$S, while the feed Se-to-S molar ratios were found to be larger than stoichiometric ratios of the resulting $PbSe_xS_{1-x}$ NCs. To obtain the homogeneously alloyed $PbSe_{0.3}S_{0.7}$ NCs, the feed molar ratio was 0.7Se-to-0.3S, in conjunction with the growth period controlled to be as short as 90 s at 150 °C. The longer the growth period, the more the Se incorporated but into the outer layers leading to a possible gradient structure. The Schottky-type solar cells based on their homogeneously alloyed $PbSe_{0.3}S_{0.7}$ NCs exhibited a power conversion efficiency (PCE) of 3.3%. The absorption peak in wavelength of the $PbSe_{0.3}S_{0.7}$ NCs seems to be in the range of 1100−1150 nm. Note that the optimal bandgap in wavelength of active materials used in solar cell devices was calculated to be in the range of ∼900−1300 nm. When the PV devices were operated at ∼1100 nm (bandgap energy E_g ∼1.1 eV), their maximum thermodynamic conversion efficiencies might be achieved.[7] For ternary $PbSe_xS_{1-x}$ NC-based Schottky-type solar cells, the NC structure (homogeneous vs gradient), composition, and size are important to accomplish high PCE.

Although (TMS)$_2$S is widely used as a S source in the synthesis of colloidal NCs, it is air sensitive, odorous, and expensive.[8,9] Furthermore, the role of DPP in eq 1 approach was not discussed and the DPP amount was not explored.

$$Pb(oleate)_2 + TOPSe + (TMS)_2S + DPP \xrightarrow{ODE} PbSeS\ QDs$$
$$((1),\ 0.2DPP\text{-}2Pb\text{-}0.7Se\text{-}0.3S),\ 150\ ^\circ C,\ 90s)$$
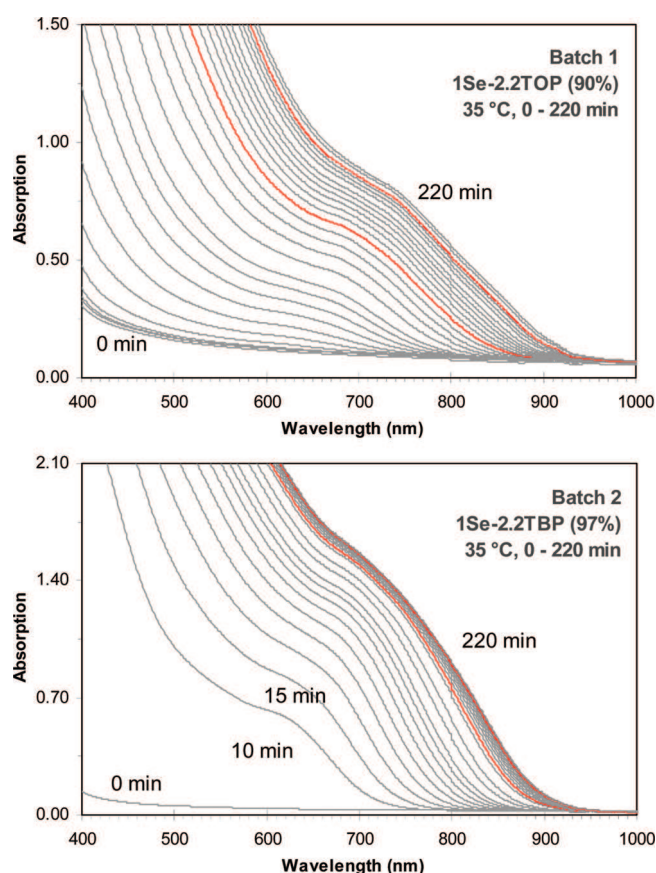
Our laboratories have been investigating the syntheses of a number of colloidal photoluminescent (PL) semiconductor QDs via a noninjection approach, which is a different synthetic protocol. Compared to the traditional hot-injection approach,[8] the noninjection approach features ready observation of nucleation with easy handling, high synthetic reproducibility, and large-scale capability. Various high-quality colloidal QDs exhibiting bright bandgap PL emission have been developed via our noninjection approach in ODE. These include II−VI, II−V, and IV−VI regular and magic-sized quantum dots (RQDs and MSQDs).[9−19] Accordingly, homogeneously alloyed $PbSe_{0.3}S_{0.7}$ NCs with a bandgap in the range of 1100−1200 nm were

developed via our noninjection low-temperature approach with long growth periods.

$$Pb(oleate)_2 + TBPSe + TAA + DPP \xrightarrow{ODE} PbSeS\ QDs$$
$$((2),\ low\ temperature\ non\text{-}injection\text{-}based\ approach)$$
$$((0.8\sim5.8)DPP\text{-}4Pb\text{-}1.5Se\text{-}0.5S),\ 60\ ^\circ C,\ 45min)$$

As represented by eq 2, the synthesis of the homogeneously alloyed $PbSe_xS_{1-x}$ NCs was explored with air-stable and low-cost S sources such as thioacetamide (TAA), aiming at their potential to advance the third generation PV devices with lower cost and higher efficiency. TAA was reported in the synthesis of NCs with various morphologies in aqueous media.[20,21] To engineer homogeneously alloyed $PbSe_xS_{1-x}$ NCs, matching the reactivity of Se and S precursors was considered first. Our experience with the formation of gradiently alloyed ZnCdS and homogeneously alloyed CdSeS NCs via a one-pot noninjection approach was further enhanced during our investigation on the synthesis of small-sized PbSe NCs with high particle yield and high quality at low temperature (such as 50 °C) with the presence of reducing agents DPP and/or n-tributylphosphine (TBP).[11,12,19] We acknowledge that the reactivity of DOPSe/TOPSe (DOPSe, dioctylphosphine selenide, represents the active compound in a TOPSe solution) was much higher than that of DOPS/TOPS and much lower than that of TAA toward Pb(oleate)$_2$. For this reason, we decided to use DBPSe/TBPSe (DBPSe, dibutylphosphine selenide, represents the active compound in a TBPSe solution) as the Se precursor to match the reactivity of the S precursor TAA. Furthermore, we determined to promote the reactivity of Pb(oleate)$_2$, used as the Pb precursor, via the formation of a Pb−P complex with the addition of DPP.[19,22−24] The advantages of using DPP with certain DPP-to-Pb feed molar ratios include to further facilitate the reactivity match and to endorse sizable nucleation at low temperatures. It is known that a high degree of monomer supersaturation can lead to the presence of a large number of nuclei and thus the formation of small-sized NCs with high particle yield.[19]
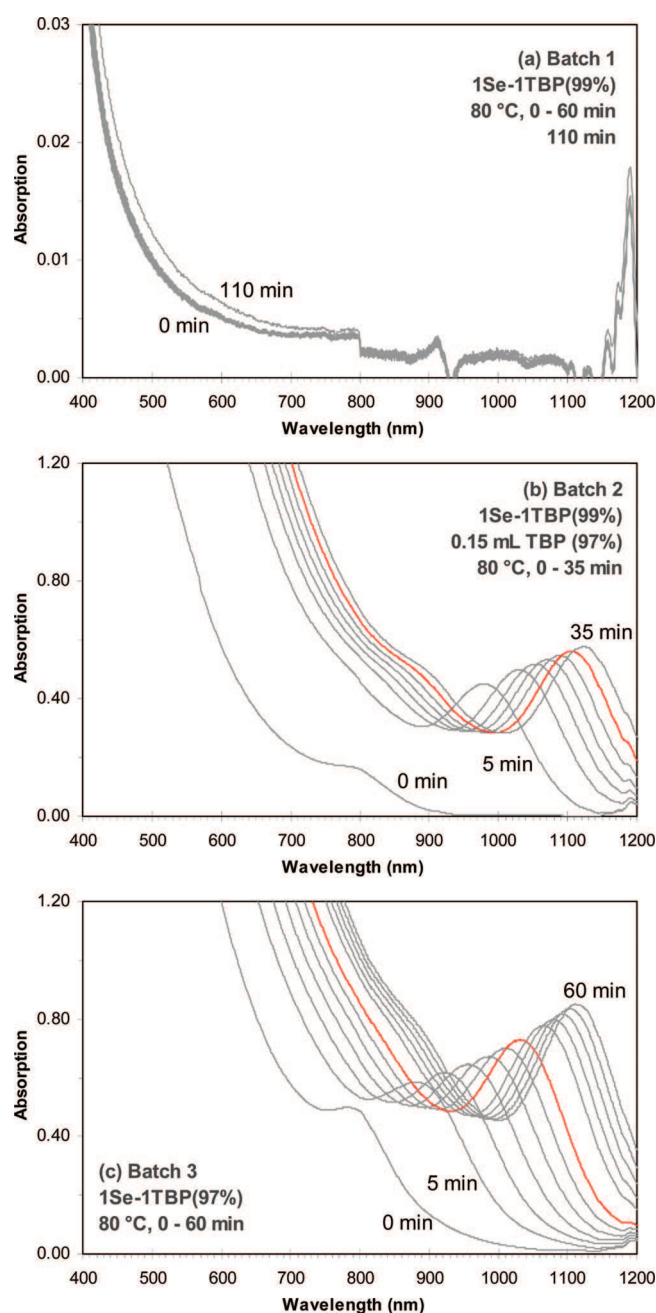
Herein, we report on the development of a noninjection one-pot approach to prepare homogeneously alloyed $PbSe_xS_{1-x}$ NCs with bandgap in the range of 1000−1200 nm, aiming at their potential in solar cell applications. This low-temperature approach which can be carried out with long growth periods is more environmentally benign and can be achieved at low-cost with the use of TAA as S source. The temporal evolution of absorption and emission of resulting $PbSe_xS_{1-x}$ NCs was monitored. Also, the $PbSe_xS_{1-x}$ NCs were characterized by transmission electron microscopy (TEM), energy-dispersive X-ray (EDX) spectroscopy, X-ray photoelectron spectroscopy (XPS), and powder X-ray diffraction (XRD). The resulting $PbSe_xS_{1-x}$ NCs are of high quality, in terms of narrow size distribution with a typical standard deviation of ∼11%, excellent optical properties with high quantum yield (QY) of ∼50−100% and small full width at half-maximum (fwhm) of ∼140−150 nm of their bandgap photoemission peaks, and long-term storage stability. Our homogeneously alloyed $PbSe_xS_{1-x}$ NCs are small-sized and excellent for solar cell applications. The Schottky-type solar cells, fabricated with our $PbSe_{0.3}S_{0.7}$ NCs as the active materials, reached a high PCE of 3.44%. The present study brings insights into the fundamental understanding of the formation mechanism of monomers and into the synthesis−structure−property−application relationship beginning with the development of composition-tunable nanocrystals.

Figure 1. Investigation on the reactivity of TOPSe (Batch 1) and TBPSe (Batch 2) via in situ observation of the temporal evolution of absorption of the PbSe NCs at 35 °C. The feed molar ratio was 1Pb-to-2.6Se for the two batches and the feed [Pb] was 187 mmol/kg for batch 1 and 50 mmol/kg for batch 2. The absorption spectra were collected at a 5-min time interval during the first 50 min followed by a 10-min time interval afterward. The growth period examined was 220 min and is indicated for each of the two batches, with the red lines signifying the growth periods of 100 and 200 min. The 5-min absorption for batch 2 was missing during in situ absorption collection. It is clear that the reactivity of TOPSe (batch 1) is lower than that of TBPSe (batch 2) under the experimental conditions.
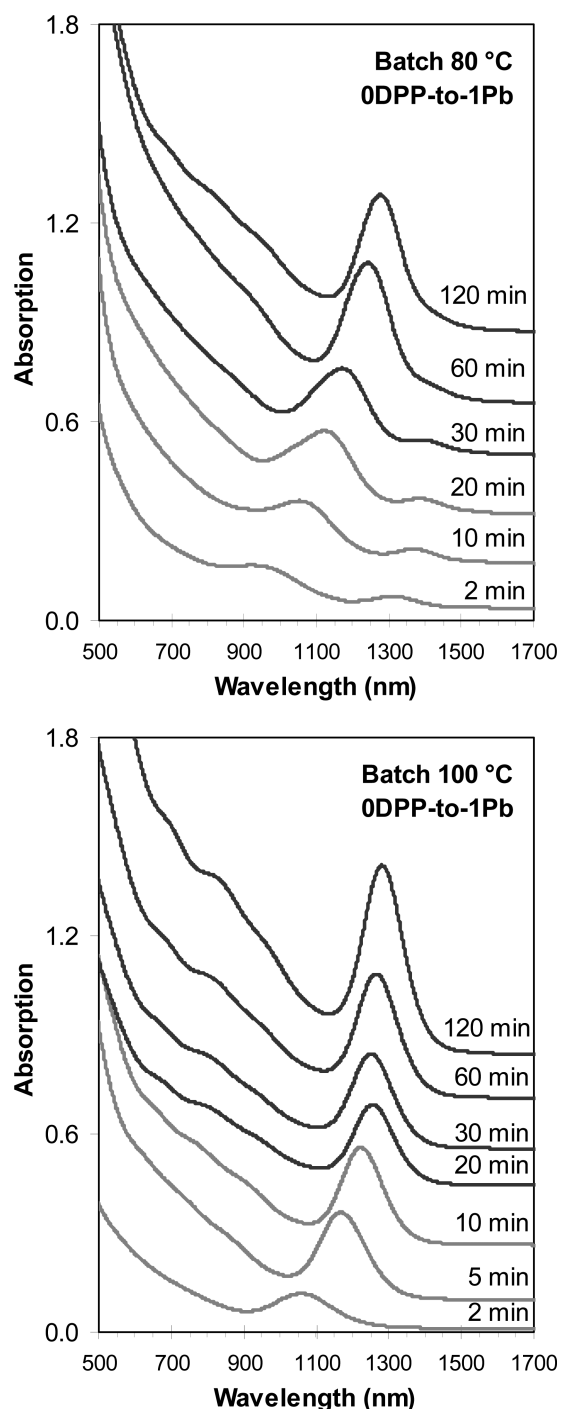
■ RESULTS AND DISCUSSION

The present study focuses on the development of the eq 2 approach, with its synthetic design concentrating on sizable nucleation at low temperature with the presence of a large number of nuclei. Accordingly, the growth could be carried out at low temperature with long reaction periods accompanied by an increase of the Se amount in the resulting $PbSe_xS_{1-x}$ NCs. We present, first, the use of commercially available TBP 97% instead of TBP 99%, following the recent argument on the tertiary phosphine selenide vs secondary phosphine selenide and the formation mechanism of monomers proposed.[19,22−24] A modified monomer formation mechanism of our approach shown by eq 2 is proposed by eqs aM and bM; the combination of the monomer leads to nucleation/growth of the correspondingly NCs. Second, the use of DPP is addressed to promote the formation of alloyed $PbSe_xS_{1-x}$ NCs at 60 °C instead of higher temperature (such as 100 °C), together with homogeneous instead of gradient alloys. Also, the DPP amount used affects the composition of the resulting $PbSe_xS_{1-x}$ NCs (at a fixed Se-to-Se feed molar ratio) and this effect is discussed. Finally, the

Figure 2. Investigation on the use of commercial TBP (97% and 99%) affecting the progression of PbSe NCs via in situ observation of the temporal evolution of absorption of the PbSe NCs at 80 °C. The feed molar ratio was 1Pb-to-2.5Se and the feed [Pb] was 87 mmol/kg for the three batches, with Se precursors of (a) 1Se-1TBP 99% feed molar ratio, batch 1, (b) 1Se-1TBP 99% feed molar ratio and additional 0.15 mL TBP 97% (corresponding to a 1Se-1TBP 99%-1.2 TBP 97% feed molar ratio), batch 2, and (c) 1Se-1TBP 97% feed molar ratio, batch 3. The absorption spectra were collected with a 5-min time interval in the first 60 min. The growth period examined is indicated for each of the three batches, with the red lines signifying the growth periods of 30 min. The 35-min absorption for batch 3 is missing. It is clear that the reactivity of batch 1 TBPSe made from TBP 99% is much lower than that of batch 3 from TBP 97%, under the experimental conditions. See Supporting Information Scheme S2 for the presence of DBPSe in batch 3 and not in batches 1 and 2.

preliminary data on the performance of our Schottky-type solar cells fabricated with the $PbSe_xS_{1-x}$ NCs are described.
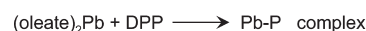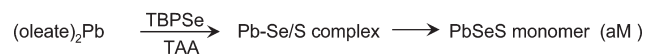
Figure 3. Investigation on the noninjection approach (eq 2) to alloyed PbSe$_x$S$_{1-x}$ NCs in the absence of DPP, via monitoring the temporal evolution of absorption (offset) of the NCs from two batches at 80 °C (top) and 100 °C (bottom). The growth temperature and periods in min are indicated. The other synthetic conditions were: a feed molar ratio of 4 Pb-to-1.5 TBPSe-to-0.5 TAA and a reactant concentration [Se + S] of ~55 mmol/kg.

Use of TBP 97% Instead of TOP 90% or TBP 99% for High Se Precursor Reactivity.

Figure 1 shows the in situ observation of the temporal evolution of absorption of the PbSe NCs from two batches. For the two batches with a 1Pb-to-2.6Se feed molar ratio, the growth temperature was 35 °C. The Pb precursor was Pb-(oleate)$_2$ prepared with a 2.2OA-to-1PbO feed molar ratio in ODE;
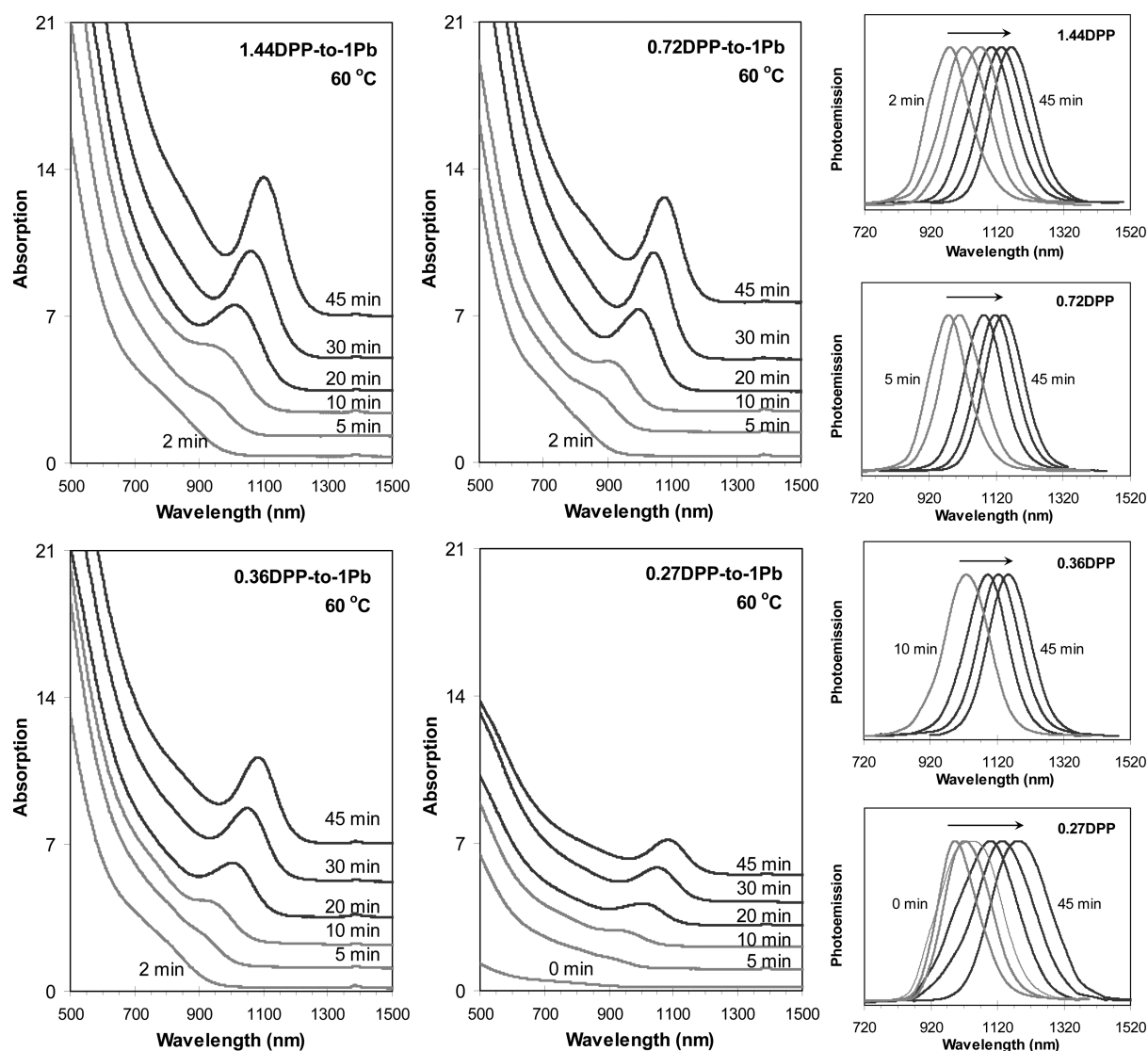
the feed [Pb] was 187 mmol/kg for batch 1 and 50 mmol/kg for batch 2. The Se precursors were DOPSe/TOPSe made with 1Se-to-2.2TOP (90%, batch 1) and DBPSe/TBPSe made with 1Se-to-2.2TBP (97% for batch 2). It is apparent that under the experimental conditions of the noninjection-based low temperature approach, the reactivity of TBPSe (batch 2) is higher than that of TOPSe (batch 1). For the Figure 1 TOPSe and TBPSe stock solutions, both DOPSe and DBPSe were not detected with ^{31}P NMR in a temperate range of 25–80 °C, respectively. See Supporting Information Scheme S1.[19]

Figure 2 shows the in situ observation of the temporal evolution of absorption of the PbSe NCs from three batches. For the three batches with a 1Pb-to-2.5Se feed molar ratio, the growth temperature was 80 °C. Again, the Pb precursor was Pb(oleate)$_2$ prepared with a 2.2OA-to-1PbO feed molar ratio in ODE, while the feed [Pb] was 87 mmol/kg for the three batches. The Se precursors were TBPSe made with a feed molar ratio of 1Se-to-1TBP 99%, (a, batch 1), 1Se-to-1TBP 99%, with 0.15 mL TBP 97% added, corresponding to total 1Se-to-1TBP 99%-to-1.2TBP 97% (b, batch 2), and 1Se-to-1TBP 97% (c, batch 3). With batch 1 TBP 99%, there was little NC presence but with the absorption from the solvent ODE. It is clear that under the experimental conditions of the noninjection-based low temperature approach, the reactivity of DBPSe/TBPSe made from TBP 97% (c, batch 3) is much higher than that made from TBP 99% (a, batch 1). Such an experimental result seems to be in agreement with the argument that pure tertiary phosphine selenide Se=PR$_{a3}$ such as TOPSe or TBPSe did not react with Pb(oleate)$_2$, but secondary phosphine selenide Se=PH(R$_a$)$_2$ such as DOPSe or DBPSe did.[19,24] Supporting Information Scheme S2 shows our corresponding ^{31}P NMR study of the three Se solutions used in the Figure 2 batches. The ^{31}P NMR spectra demonstrate that no DBPSe was detected in Batch 1 SeTBP 99% solution and in Batch 2 solution, while DBPSe was detected in Batch 3 SeTBP 97% solution. Furthermore, the presence of additional TBP (97%) in Batch 2 promoted the reactivity of Pb(oleate)$_2$.[19] Such an experimental result seems to be in agreement with the existence of a reducing pathway (accompanied with the occurrence of a Pb—P complex which should be much more reactive than Pb(oleate)$_2$). This concept is represented by eq (bM) where DPP was used instead of TBP 97%.[19,22,23]

Accordingly, for the present synthesis of homogeneously alloyed PbSe$_x$S$_{1-x}$ with low-cost and air-stable TAA as the S precursor, we selected TBP 97% to prepare the Se precursor TBPSe (with the feed molar ratio of 1 Se-to-2.2 TBP). Also, we used DPP as a reducing agent to promote the formation of Pb—P complex which exhibited much higher reactivity than Pb(oleate)$_2$ and thus to further tune the reactivity match of the Se and S precursors at low temperature. Supporting Information Scheme S3 shows the ^{31}P NMR spectra from a mixture of Pb(oleate)$_2$ and DPP. For our low-temperature approach shown by eq 2, we propose a modified mechanism for the formation of the monomer by below eqs aM and bM. The combination of the monomer led to nucleation/growth of homogeneously alloyed PbSe$_x$S$_{1-x}$ NCs.

DPP Effects on the Formation of Homogeneously Alloyed PbSe$_x$S$_{1-x}$ NCs.
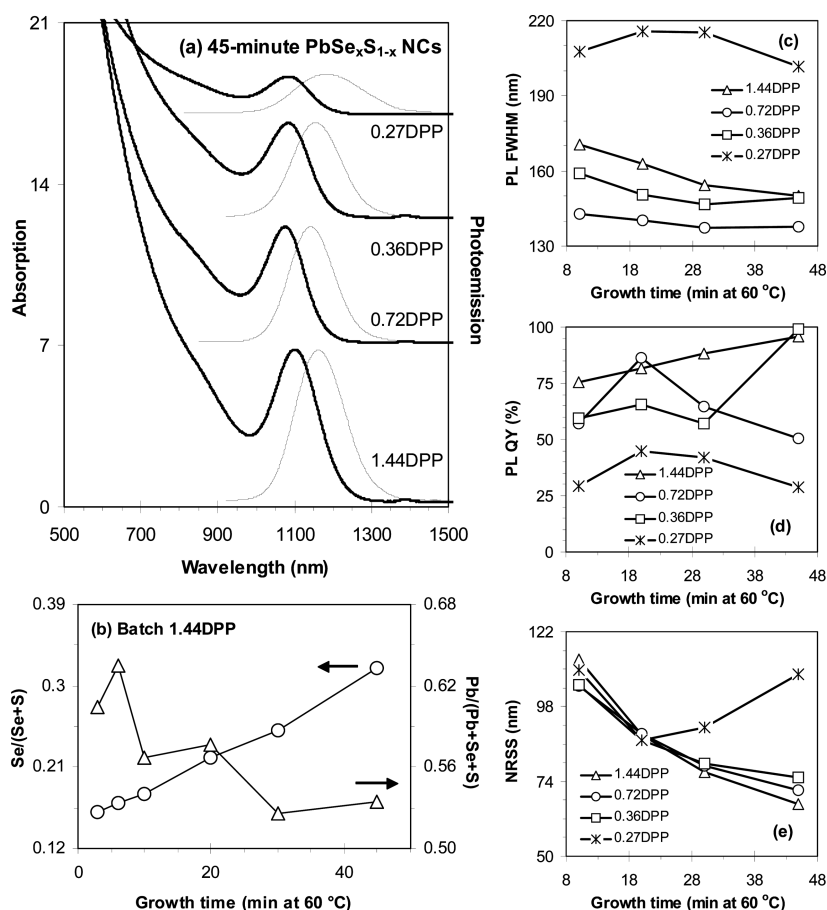
Without the presence of DPP in our noninjection

Figure 4. Investigation on the effect of DPP amounts affecting the growth of PbSe$_x$S$_{1-x}$ NCs from four noninjection batches at 60 °C via monitoring the temporal evolution of their optical properties. The absorption spectra (offset, left and middle panels) were normalized to 1.0 g of crude growth mixtures and dispersed in 1.0 mL TCE; the corresponding emission spectra (right panel) were normalized. The growth periods at 60 °C in min are indicated. The other synthetic conditions were: a feed molar ratio of 4Pb-to-1.5TBPSe-to-0.5TAA and a reactant concentration [Se + S] of ~55 mmol/kg.

approach depicted by eq 2, the growth temperature needs to be higher than 80 °C. Figure 3 shows the temporal evolution of absorption (offset) of the NCs from two batches in the absence of DPP. For these two "controlled" batches, the feed molar ratio was 4Pb-to-1.5TBPSe-to-0.5TAA and the feed [Se+S] was ~55 mmol/kg, while the growth temperature was 80 °C (top) and 100 °C (bottom). The growth periods monitored were from 2 to 120 min. For batch 80 °C with 2-min growth, there were two NC ensembles, as indicated by two absorption peaks. Along with the reaction/growth, both absorption peaks red-shifted. Accordingly, the reactivity of TBPSe and TAA in ODE did not seem to match well, but leading to inhomogeneous nucleation with the growth of two ensembles. For Batch 100 °C, there was one NC ensemble (even at 2-min growth monitored) with its absorption peak red-shifting along the reaction/growth. The reactivity of TBPSe and TAA in ODE seemed to match better, leading to the presence of homogeneous nucleation and the absence of inhomogeneous nucleation. Therefore, the growth temperature should be higher

than 80 °C for the presence of homogeneous nucleation from the eq 2 approach when DPP is absent.

In the absence of DPP, we failed to obtain PbSe$_{0.3}$S$_{0.7}$ NCs with a homogeneously alloyed structure. Due to the relatively high reactivity of TAA, the amount of Se in the resulting PbSe$_x$S$_{1-x}$ NCs is much lower than its feed amount. For instance, the 120-min-growth ensemble of Batch 80 °C was PbSe$_{0.07}$S$_{0.93}$ and the 60-min-growth ensemble in Batch 100 °C was PbSe$_{0.14}$S$_{0.86}$ (as determined by XPS). Our efforts to synthesize homogeneously alloyed PbSe$_{0.3}$S$_{0.7}$ NCs through the increase of the feed Se-to-S or Pb-to-(Se + S) molar ratios failed. When the amount of Se increased, Se deposited on the outer layers leading to a gradient structure rather than a homogeneous structure. For instance, a 60-min-growth ensemble from a batch with a feed molar ratio of 8Pb-to-1.9TBPSe-to-0.1TAA was determined to be PbSe$_{0.72}$S$_{0.28}$ (XPS) or PbSe$_{0.54}$S$_{0.46}$ (EDX). Note XPS is relatively sensitive to surface, while EDX to the bulk. A Schottky-type solar cell fabricated with this ensemble as its active materials exhibited a PCE of 1.31%.
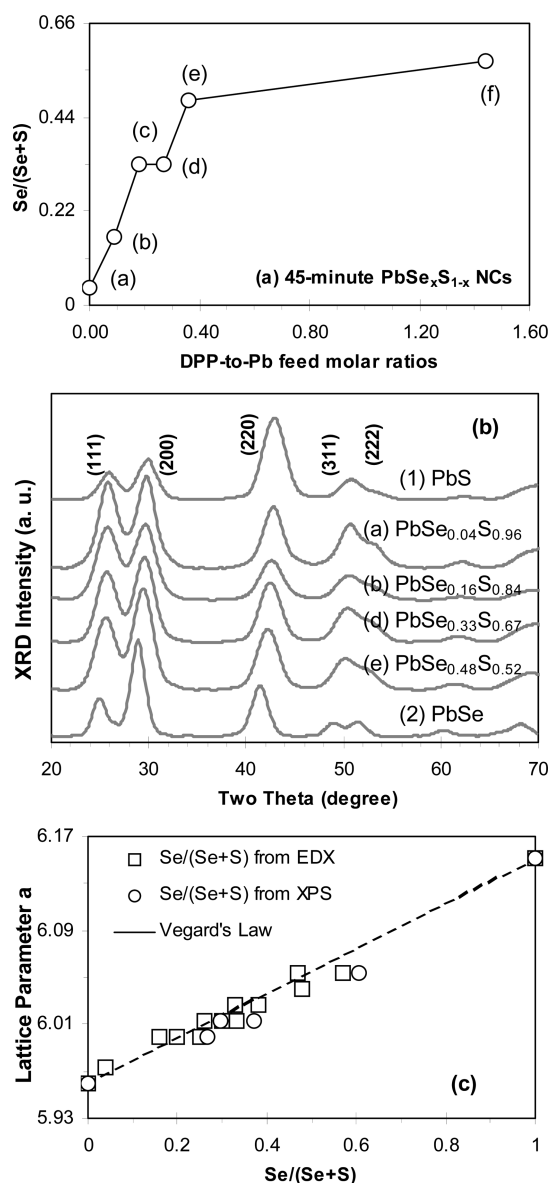
Figure 5. Investigation on the effect of DPP amounts affecting the growth of PbSe$_x$S$_{1-x}$ NCs. (a) Comparison of the optical properties of the 45-min PbSe$_x$S$_{1-x}$ NCs from the four batches shown in Figure 4. (b) The change of the composition of the resulting PbSe$_x$S$_{1-x}$ NCs from Figure 4 Batch 1.44DPP. Summary of the change of PL fwhm (c), PL QY (d), and NRSS (e) of the PbSe$_x$S$_{1-x}$ NCs from the four batches shown in Figure 4.

On the other hand, the presence of DPP enhances Route (bM);[19,22] therefore, the growth temperature can be reduced and homogeneous PbSe$_x$S$_{1-x}$ NCs with tunable Se composition can be achieved readily. Figure 4 illustrates the temporal evolution of the optical properties of the PbSe$_x$S$_{1-x}$ NCs from four synthetic batches at 60 °C. For the four batches presented to illustrate the effect of DPP amounts, the feed molar ratio was 4Pb-to-1.5TBPSe-to-0.5TAA and the feed [Se + S] was ~55 mmol/kg. The feed DPP amounts are addressed as the feed (1.44, 0.72, 0.36, and 0.27)DPP-to-1Pb molar ratios, together with the growth periods monitored up to 45 min. During the growth periods monitored, the redshifts of absorption and photoemission were obvious. It is evident that the larger the DPP-to-Pb feed molar ratio, the earlier the nucleation, and the greater the number of the nanocrystals. Interestingly, the 45-min NCs from Batches 1.44, 0.72, 0.36, and 0.27DPP-to-1Pb exhibited different (EDX) Se compositions of 0.47, 0.38, 0.32, and 0.20, but similar first exciton absorption/emission peak positions at 1099/1166, 1074/1145, 1082/1157, and 1081/1190 nm, respectively. The absorption of the 45-min NCs is close to the optimal bandgap of ~1100 nm for solar cell applications.[5,7]

Figure 5a presents the comparison of the absorption and emission of the 45-min PbSe$_x$S$_{1-x}$ ensembles from the four batches. The absorption spectra (solid lines) were offset and normalized to 1.0 g of crude growth mixtures and dispersed in 1.0 mL TCE, while the emission spectra (dashed lines) were

normalized accordingly. Again, the DPP feed amounts are indicated as DPP-to-1Pb feed molar ratios. The Se/(Se + S) atomic number ratios of the 45-min PbSe$_x$S$_{1-x}$ NCs (from the top to bottom batches) were increased from 0.20 to 0.47 as studied by EDX. Therefore, it is easy to tune the composition of the resulting homogeneously alloyed PbSe$_x$S$_{1-x}$ NCs with the addition of different amounts of DPP. The evidence of a homogeneous versus gradient structure is demonstrated in the bottom part of Figure 6.[11,12] Here, the larger the DPP-to-Pb feed molar ratio, the more the Se/(Se + S) molar ratio of the resulting nanocrystals. Moreover, there is an increase of the Se/(Se + S) molar ratio along the reaction; one example is shown in Figure 5b. The increase of the Se/(Se + S) molar ratio along the reaction is appreciable, together with the fact that the PbSe$_x$S$_{1-x}$ NCs were Pb-rich.

Moreover, the PbSe$_x$S$_{1-x}$ NCs from batches 0.36 DPP and 0.72 DPP exhibited relatively small PL full width at half-maximum (fwhm), as shown in Figure 5c. The PbSe$_x$S$_{1-x}$ NCs from Batch 0.27 DPP exhibited relatively small PL QY, as shown in Figure 5d. Interestingly, the PbSe$_x$S$_{1-x}$ NCs from Batches 0.36 DPP, 0.72 DPP, and 1.44 DPP exhibited a decrease of non-resonant Stokes shift (NRSS, the energy difference between the bandgap absorption and emission) along the reaction, as shown in Figure 5e. For the 45-min PbSe$_x$S$_{1-x}$ NCs from the four batches with an increase of the DPP amount from 0.27 DPP to 1.44 DPP, there is a decrease of the NRSS, together with an

Figure 6. (a) Investigation on the Se molar composition affected by different DPP amounts used. (b) Powder XRD patterns of binary PbS and PbSe NCs, and ternary $PbSe_xS_{1-x}$ NCs (of batches a, b, d, and e shown in a). (c) The dependence of the lattice parameter a (in Å) on the Se molar composition x in the $PbSe_xS_{1-x}$ NCs.

increase of their Se/(Se + S) atomic number ratios from 0.20 to 0.47.

It is worth noting that the experimental parameters and the interplay between them affect the composition, as well as growth kinetics of the resulting $PbSe_xS_{1-x}$ NCs. In particular, the amount of DPP plays an important role in tuning the composition of the $PbSe_xS_{1-x}$ NCs from the eq 2 approach. To explore the synthetic window for the fabrication of homogeneously alloyed $PbSe_{0.3}S_{0.7}$ NCs, the syntheses were carried out at 60 °C but without intermediate sampling during the 45-min growth periods. For the six batches shown in Figure 6a, the feed molar ratio was 4Pb-to-1.5TBPSe-to-0.5 TAA and the feed [Se + S] was ∼55 mmol/kg, with different feed molar ratios of 0DPP-to-1Pb (Batch a), 0.09-DPP-to-1Pb (Batch b), 0.18DPP-to-1Pb (Batch c), 0.27DPP-to-1Pb (Batch d), 0.36DPP-to-1Pb (Batch e), and 1.44DPP-to-1Pb
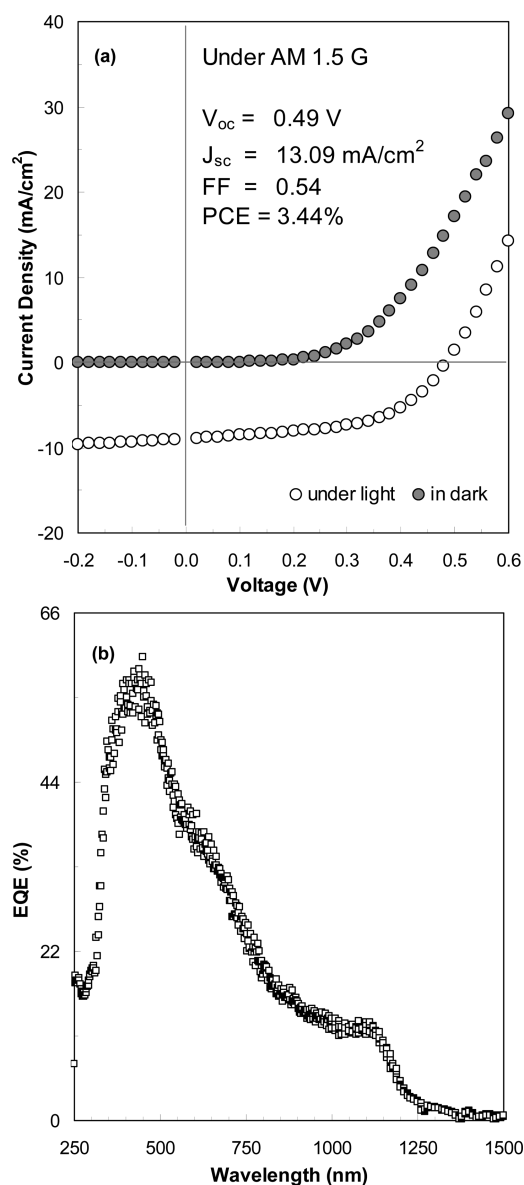
(Batch f). The 45-min NCs exhibited absorption peaking at 1336 nm, 1120 nm, 1131 nm, 1129 nm, 1138 nm, and 1124 nm, respectively. Meanwhile, the Se/(Se + S) molar compositions of the corresponding 45-min $PbSe_xS_{1-x}$ NCs (from the six batches without intermediate sampling) were measured by EDX; the Se molar compositions were 0.04, 0.16, 0.33, 0.33, 0.48, and 0.57, respectively. Thus, the Se molar composition was tuned from 0.04 to 0.57, when the DPP-to-1Pb feed molar ratio was increased from 0 to 1.44. The feed molar ratio of $(0.2-0.3)$DPP-to-1Pb seems to offer a superior synthetic window for the fabrication of homogeneously alloyed $PbSe_{0.3}S_{0.7}$ NCs via the eq 2 approach for photovoltaic applications.

The powder XRD patterns of the $PbSe_xS_{1-x}$ NCs from batches a, b, d, and e are presented in Figure 6b, together with those measured from binary PbS (Curve 1) and PbSe (Curve 2) NCs. The XRD study supports the formation of ternary-alloyed $PbSe_xS_{1-x}$ NCs and demonstrates their crystal structures to be cubic rock salt. The binary PbS and PbSe NCs used exhibited absorption peaking at 1119 and 1590 nm, respectively. The lattice parameter a of the ternary $PbSe_xS_{1-x}$ was then calculated from the XRD patterns based on (220) diffraction peaks. Afterward, the relationship between the lattice parameter a and the Se/(Se + S) molar composition was plotted and shown in Figure 6c. The Se/(Se + S) molar compositions obtained from EDX are represented by open square symbols, while those from XPS by open circular symbols. The dashed linear line symbolizes the Vegard's law, with the lattice parameter a of our PbSe NCs (where $x = 1$) calculated to be 6.15 Å from one ensemble exhibiting absorption peaking at 1221 nm, and that of our PbS NCs (where $x = 0$) 5.96 Å from one ensemble peaking at 1154 nm. It is understandable that our $PbSe_xS_{1-x}$ NCs (where x up to 0.5) are homogeneously alloyed instead of gradiently alloyed.

In addition to XRD and XPS, the $PbSe_xS_{1-x}$ NCs were studied by TEM, as illustrated in Supporting Information Figure S1. Their size distribution is narrow. The size of a typical ensemble of $PbSe_{0.33}S_{0.67}$ NCs (with its first exciton peaking at 1143 nm as shown in Figure S1B) was measured from the TEM images shown in Figure S1A and is presented in Figure S1B. The resulting mean size was measured to be 4.41 ± 0.50 nm, with a standard deviation of ∼11%. Also, the mean size was estimated by Scherrer equation,[25] which is 3.32 nm by (220) plane, 3.95 nm by (111) plane, and 3.92 nm by (200) plane (see XRD spectrum Figure 6b curve d). It is acknowledged that discrepancy exists in size determination among various methods or different research groups.[19,26,27]

The comparison of the growth kinetics of PbSe, PbS and $PbSe_xS_{1-x}$ NCs from the eq 2 approach is shown in Supporting Information Figure S2. It is clear that with the use of DPP, the eq 2 approach is excellent for the formation of ternary $PbSe_xS_{1-x}$ NCs at 60 °C. Furthermore, the comparison on the temporal evolution of the optical properties of the NCs also demonstrates the formation of ternary instead of binary NCs under our experimental conditions. The excellent storage stability of the ternary $PbSe_xS_{1-x}$ NCs from the batches shown in Figure 4 is presented in Supporting Information Figure S3. Consequently, it is conceivable that our eq 2 approach with long growth periods (45 min instead of 90 s) at low temperature (60 °C instead of 150 °C) is practical for the formation of homogeneously alloyed $PbSe_{0.3}S_{0.7}$ NCs for PV applications which require large amounts of NC products.

Preliminary Study on NC-Based Schottky-Type Solar Cells. The potential of our low temperature NC products in the solar

Figure 7. (a) Current density—voltage (J—V) characteristics of a homogeneously alloyed $PbSe_{0.3}S_{0.7}$ NC-based Schottky-type solar cell under AM 1.5G irradiation of 100 mW/cm^2. The device parameters are listed. (b) The external quantum efficiency (EQE) spectrum of the solar cell.

cell application was examined using a Schottky-type diode configuration. Figure 7 displays an example of the J—V curve (a) and external quantum efficiency (EQE) spectrum (b) of a Schottky-type solar cell fabricated with our homogeneously alloyed $PbSe_{0.3}S_{0.7}$ NCs, for example. This NC ensemble exhibited its first excitonic absorption peaking at 1146 nm. For the EQE spectrum, there are two noticeable peaks; one at ~450 nm, the other at ~1110 nm. At the 450 nm peak, the EQE reached a maximum of ~60%. The 1110 nm peak manifested an effective utilization of solar energy in the near-IR region. Values of V_{oc} and fill factor (FF) were extracted to be 0.49 V and 0.54, respectively, from the J—V curve, while J_{sc} of 13.09 mA/cm^2 was calculated from the EQE spectrum. These values resulted in a PCE of 3.44%. To avoid spectral mismatch of the solar simulator for the PCE calculation, the J_{sc} value from the EQE spectrum was used instead of that of the J—V curve. It is worth noting that the values

of 13.09 mA/cm^2 J_{sc}, 0.49 V V_{oc}, and 0.54 FF are comparable to those obtained from the best $PbSe_{0.3}S_{0.7}$ NC-based Schottky-type solar cells, which were 14.8 mA/cm^2 J_{sc}, 0.45 V V_{oc}, and 0.50 FF.[3]

It was documented that the optimal composition of homogeneously alloyed $PbSe_xS_{1-x}$ NCs was $PbSe_{0.3}S_{0.7}$, and a corresponding Schottky-type solar cell fabricated exhibited a PCE of 3.3%.[3] Our PV study with our low-cost NCs via a low-temperature noninjection-based approach is in agreement with such a conclusion on the composition and device performance relationship. Relevant information on the performance of our $PbSe_xS_{1-x}$-based solar cells is presented in Supporting Information Table S1 and Figure S4.

■ CONCLUSION

We have developed a low-temperature noninjection-based approach to produce composition-tunable homogeneously alloyed $PbSe_xS_{1-x}$ NCs with high quality, high synthetic reproducibility, and high particle yield. Typically, the synthesis was carried out in ODE at 60 °C with the presence of diphenylphosphine (DPP). The Pb precursor was Pb(oleate)$_2$ made from PbO and oleic acid, while the Se precursor was TBPSe made from elemental Se and commercially available TBP 97% instead of TBP 99%. To the best of our knowledge, the present study is the first using an air-stable and low-cost S source, thioacetamide (TAA), to synthesize homogeneously alloyed $PbSe_xS_{1-x}$ NCs in ODE with long growth periods at low temperature. The amount of DPP used is an important parameter, tuning the composition of the resulting $PbSe_xS_{1-x}$ NCs via the promotion of the reactivity match of TBPSe and TAA. The presence of DPP promoted the formation of a Pb—P complex, which is much more reactive than Pb(oleate)$_2$, and increased the reactivity of TBPSe more than that of TAA. The larger the DPP-to-Pb feed molar ratio, the more the Pb—P complex, the higher the Se amount in the resulting homogeneously alloyed $PbSe_xS_{1-x}$ NCs. Thus, the novelty of the present study also lies in the ready tuning of the Se composition of the NCs, with the amount of DPP used. Our homogeneously alloyed $PbSe_{0.3}S_{0.7}$ NCs have demonstrated very promising results in our preliminary testing of Schottky-type solar cell devices. The best device reached a high PCE of 3.44%, with V_{oc} = 0.49 V, J_{sc} = 13.09 mA/cm^2, and FF = 0.54.

■ EXPERIMENTAL METHODS

All chemicals used are commercially available from Sigma-Aldrich (or otherwise specified) and were used as received. They were PbO (99.999%), oleic acid (OA, tech. 90%), 1-octadecene (ODE, tech. 90%), selenium (Se ~200 mesh, 99.999%, Alfa Aeser), thioacetamide (TAA, ≥99%), n-trioctylphosphine (TOP, tech. 90%), n-tributylphosphine (TBP, 97%), n-tributylphosphine (TBP, 99%, Strem chemical company), diphenylphosphine (DPP, 98%), tetrachloroethylene (TCE, ≥99%, spectrophotometric grade), 1,2-dichloroethane (≥99%, spectrophotometric grade), and dye IR 26 (Exciton). Solvents used for purification were toluene (99.5%, ACS reagent, ACP in Montreal), hexane (98.5%, GR ACS, EMD in USA), methanol (absolute, ACP in Montreal), and acetone (99.5%, ACS reagent). Also, anhydrous solvents were used for the purification carried out in a glovebox of our NCs used for PV devices; they were toluene (99.8%), hexane (99%), methanol (99.8%), and acetone (spectrograde, ACP in Montreal, dried with 4 Å molecular sieves).

To make a 0.681 mmol/g Pb(oleate)$_2$ stock solution, 6.0085 g (26.92 mmol) PbO, 17.028 g (60.19 mmol, without the consideration of 90% purity) oleic acid, and 16.976 g ODE were placed in a 3-necked 100-mL round-bottom flask equipped with an air-condenser and a

thermocouple. Note that for reactions carried out in flasks, standard air-free techniques were used throughout all syntheses. Here, the mixture was degassed at room temperature under vacuum until no vigorous bubbling, and then heated up to ~180 °C under purified nitrogen until PbO was all dissolved resulting in a clear solution. Afterward, the mixture was cooled down to ~110 °C and was degassed (~50 mtorr) again for 1 h. Under N_2 protection, the mixture was finally cooled down to room temperature.

To make TOPSe and TBPSe stock solutions of (1) 1Se-to-2.2TOP (TOP 90%), (2) 1Se-to-2.2TBP (TBP 97%), (3) 1Se-to-3.5TBP (TBP 97%), (4) 1Se-to-1TBP (TBP 97%), (5) 1Se-to-1TBP (TBP 99%), Se powder and TOP or TBP in the specified molar ratios (without the consideration of TOP and TBP purities) were added into single-necked 25-mL flasks in glovebox filled with N_2. The mixtures were then stirred at room temperature overnight. The solutions (1)−(3) became clear and were ready. The TBPSe solutions 4 and 5 were then heated gently for ~10 min to ensure a complete reaction between TBP and Se. All the TOPSe and TBPSe stock solutions were kept in the glovebox.

For in situ observation reactions, a typical synthesis was started in a glovebox under N_2 atmosphere. A $Pb(oleate)_2$ stock solution, a Se precursor stock solution, and ODE were added into a quartz cuvette (optical path 10 mm × 10 mm, volume 3.5 mL) at room temperature and then sealed with a Teflon stopper. ODE was dried previously by degassing (at ~50 mtorr and ~100 °C) and purging with purified nitrogen three times within two hours. The total volume of the chemicals was kept as ~2.9 mL. The cuvette was then transferred out of the glovebox and placed into Cary 5000 for the study of the reactivity of the Se precursor made from 90% TOP, 97% TBP, and 99% TBP.

For a typical synthesis of homogeneously alloyed $PbSe_xS_{1-x}$ NCs via our one-pot noninjection-based synthetic protocol (such as shown in Figure 4 batch 0.36DPP), 0.3645 g (1.6 mmol) PbO, 1.145 g (4.0 mmol) oleic acid (OA), and 8.01 g ODE were placed in a 3-necked 100-mL round-bottom flask equipped with an air-condenser and a thermocouple. The mixture was degassed at room temperature under vacuum until no vigorous bubbling was observed, and then heated to ~180 °C under N_2 until PbO was completely dissolved. Afterward, this $Pb(oleate)_2$ solution was degassed (at ~50 mtorr) again for 1 h at ~110 °C, and then cooled down to ~30 °C under N_2. 15.6 mg (0.2 mmol) TAA and ODE 2.5 g were loaded in a 1-dram vial and sonicated for 1 h to get a fine powder suspension, which was then transferred into the flask containing a $Pb(oleate)_2$ solution; ~1.0 g ODE was used to rinse the vial. The mixture was degassed at 30−35 °C under vacuum and then purged with N_2 three times in 30 min, then 100 μL (0.56 mmol) DPP and 0.6 mmol TBPSe (1Se-to-3.5TBP, TBP 97%) stock solution, which were mixed and diluted with ~2.0 mL dry ODE, were added into the flask. Afterward, the mixture was heated up under N_2 to the desired temperature such as 60 °C with a temperature increase rate of ~10 °C/min. Therefore, the feed molar ratios for such a batch were 2.5OA-to-1Pb, 0.36DPP-to-1Pb, and 4Pb-to-1.5TBPSe-0.5TAA, together with the [Se + S] of ~53 mmol/kg in a ~15 g reaction medium.

To monitor the temporal evolution of absorption, small amounts (~1 g) of aliquots were quickly taken out of the reaction flask. Each sample was weighed and then dispersed in toluene and precipitated with methanol, and centrifuged. The precipitates were dispersed again in toluene and precipitated with methanol, and centrifuged. Afterward, the precipitates were further dispersed in hexane and precipitated with acetone (if needed, a small amount of methanol was added to cause complete precipitation of the NCs). The purified samples were dried by a fast flow of nitrogen, and then dispersed in 1.0 mL TCE. To minimize any possible change of the NCs, optical measurements were carried out immediately for the purified samples dispersed in 1.0 mL TCE at room temperature.

Ultraviolet−visible-near-infrared (UV−vis-NIR) absorption spectra were collected with a Cary 5000 spectrophotometer using a 1-nm data

interval. Quantitative dilution was performed, when the sample dispersion was too concentrated.

Near-IR PL emission spectra were collected with a HORIBA JOBIN YVON Fluorolog-3 model FL3−11 spectrofluorometer, equipped with 2 mm diameter InGaAs photodiode whose operating temperature was at −196 °C with the working range of 1000−1500 nm. Both the entrance and exit slits were 3 nm and data increment was 1 nm. Dilute NC dispersions in TCE were used, with ~0.1 optical density (O. D.) at the excitation wavelength used. Origin 8 was used for the integration with baseline subtraction and Gaussian fitting, to obtain the information on emission peak position, fwhm, and area (intensity). The PL QY was estimated by comparing the sample emission intensity with that of IR26 dye in dichloroethane (lit. QY 0.5%).[28] Corrections were made for the difference of the refractive index of the two solvents and for the detector response sensitivity.

^{31}P NMR was performed on a Bruker AV-III 400 spectrometer operating at 161.98 MHz for ^{31}P. An external standard 85% H_3PO_4 was used. The samples were prepared in a glovebox with feed molar ratios of (1) 1Se-to-1TBP 99%, (2) 1Se-to-1TBP 97%, and (3) 1Pb-$(oleate)_2$-to-1DPP. The NMR measurements were carried out in the temperature range of 25−80 °C.

Intense purification of our NCs was carried out for the characterization of X-ray photoelectron spectroscopy (XPS), powder X-ray diffraction (XRD), and transmission electron microscopy (TEM). XPS was performed using a Kratos Axis Ultra XPS equipped with a monochromated Al X-ray source. The takeoff angle was 54°. The purified NCs were deposited and dried on silicon wafer substrates, which were then mounted directly to a sample holder. All analyses were calibrated to C 1s at 285 eV. XRD samples were prepared by depositing the purified NCs on low-background quartz plates. XRD patterns were recorded at room temperature on a Bruker Axs D8 X-ray diffractometer using Cu K$_\alpha$ radiation in a $\theta-\theta$ mode. The generator was operated at 40 kV and 40 mA, and data were collected between 5° and 80° in 2θ with a step size of 0.1° and a counting time of 5 s per step. TEM samples were prepared by depositing dilute purified NC dispersions in TCE or hexane onto 400-mesh thin-carbon-coated copper grids, together with air-dry. TEM images were collected on a JEOL JEM-2100F electron microscope operating at 200 kV and equipped with a Gatan UltraScan 1000 CCD camera. The NC size and standard deviation were obtained by analyzing >1000 individual NCs with the Gatan Digital Micrograph built-in statistics function.

For the fabrication of NC-based Schottky-type solar cells with a structure of ITO (Indium tin oxide)/NCs/LiF (1 nm)/Al (100 nm), prepatterned ITO glass substrates were cleaned in an ultrasonic bath stepwise by acetone and isopropanol. Before use, the cleaned substrates were treated further with UV-ozone for 15 min. For the active layers of NCs, they were prepared by a sequential layer-by-layer cross-linking technique. First, a 5 mg/mL solution of purified NCs in chloroform was spin-cast onto the top of an ITO substrate at 5000 rpm, leading to the formation of a film with a thickness of 7−9 nm, corresponding to 1−2 monolayers of the NCs. Then the substrate was soaked into a 0.02 M 1,3-benzenedithiol (BDT) solution in acetonitrile for 30 s to replace oleic acid with BDT. The substrate was taken out and spun at 5000 rpm for 1 min to have a speedy drying process. Such a procedure was repeated to achieve a desired NC film thickness. Finally, the LiF/Al electrode was evaporated thermally on top of the NC film. Note that the preparation of the active layer was performed in a glovebox filled with dry nitrogen, together with device testing. The $J-V$ characteristics were measured with a Keithley 2400 source meter under a simulated air mass 1.5G (AM 1.5G) and solar irradiation of 100 mW/cm^2. The EQE data were acquired with a customer made setup consisting of a Jobin-Yvon Triax 180 spectrometer, a Jobin-Yvon xenon light source, a Merlin lock-in amplifier, a calibrated Si detector, and a SR 570 low noise current amplifier.

■ ASSOCIATED CONTENT

ⓢ Supporting Information. ^{31}P NMR study of SeTOP 90%, SeTBP 99%, SeTBP 97%, and a mixture of Pb(oleate)$_2$ with DPP, TEM images and size/size distribution determined by TEM and XRD of the PbSe$_{0.33}$S$_{0.67}$ NCs from our noninjection-based low temperature approach, the methods used to determine the compositions and standard deviations, comparison of the growth of the PbSe, PbS, and PbSe$_x$S$_{1-x}$ NCs under identical conditions with the presence of DPP, the storage stability of our PbSe$_x$S$_{1-x}$ NCs synthesized, and device data of Schottky-type solar cells fabricated with our PbSe$_x$S$_{1-x}$ NCs with varied Se compositions. This material is available free of charge via the Internet at http://pubs.acs.org.

■ AUTHOR INFORMATION

Corresponding Author
*Phone: 1-(613) 993-9273. E-mail: kui.yu@nrc.ca.

■ ACKNOWLEDGMENT

■ REFERENCES

(1) Luther, J. M.; Law, M.; Beard, M. C.; Song, Q.; Reese, M. O.; Ellingson, R. J.; Nozik, A. J. *Nano Lett.* **2008**, *8*, 3488–3492.

(2) Hillhouse, H. W.; Beard, M. C. *Curr. Opin. Colloid Interface Sci.* **2009**, *14*, 245–259.

(3) Ma, W.; Luther, J. M.; Zheng, H.; Wu, Y.; Alivisatos, A. P. *Nano Lett.* **2009**, *9*, 1699–1703.

(4) Tsang, S.-W.; Fu, H.; Ouyang, J.; Zhang, Y.; Yu, K.; Lu, J.; Tao, Y. *Appl. Phys. Lett.* **2010**, *96*, 243104.

(5) Kang, I.; Wise, F. W. *J. Opt. Soc. Am. B* **1997**, *14*, 1632–1646.

(6) Wise, F. W. *Acc. Chem. Res.* **2000**, *33*, 773–780.

(7) Buhl, M. L., Jr.; Bird, R. E.; Bilchak, R. V.; Connolly, J. S.; Bolton, J. R. *Solar Energy* **1984**, *32*, 75–84.

(8) Murray, C. B.; Noms, D. J.; Bawendi, M. G. *J. Am. Chem. Soc.* **1993**, *115*, 8706–8715.

(9) Liu, T.-Y.; Li, M.; Ouyang, J.; Zaman, Md. B.; Wang, R.; Wu, X.; Yeh, C.-S.; Lin, Q.; Yang, B.; Yu, K. *J. Phys. Chem. C* **2009**, *113*, 2301–2308.

(10) Ouyang, J.; Kuijper, J.; Brot, S.; Kingston, D.; Wu, X.; Leek, D. M.; Hu, M. Z.; Yu, K. *J. Phys. Chem. C* **2009**, *113*, 7579–7593.

(11) Ouyang, J.; Ratcliffe, C. I.; Kingston, D.; Wilkinson, B.; Kuijper, J.; Wu, X.; Ripmeester, J. A.; Yu, K. *J. Phys. Chem. C* **2008**, *112*, 4908–4919.

(12) Ouyang, J.; Vincent, M.; Descours, P.; Boivineau, T.; Kingston, D.; Zaman, Md. B.; Wu, X.; Yu, K. *J. Phys. Chem. C* **2009**, *113*, 5193–5120.

(13) Ouyang, J.; Zaman, B.; Yan, F.; Johnston, D.; Li, G.; Wu, X.; Leek, M. D.; Ratcliffe, C. I.; Ripmeester, J. A.; Yu, K. *J. Phys. Chem. C* **2008**, *112*, 13805–13811.

(14) Wang, R.; Ouyang, J.; Nikolaus, S.; Brestaz, L.; Zaman, Md. B.; Wu, X.; Leek, M. D.; Ratcliffe, C. I.; Yu, K. *Chem. Commun.* **2009**, 962–964.

(15) Li, M.; Ouyang, J.; Ratcliffe, C. I.; Pietri, L.; Wu, X.; Leek, D. M.; Moudrakovski, I.; Lin, Q.; Yang, B.; Yu, K. *ACS Nano* **2009**, *3*, 3832–3838.

(16) Yu, K.; Ouyang, J.; Zaman, B.; Johnston, D.; Yan, F.; Li, G.; Ratcliffe, C. I.; Leek, M. D.; Wu, X.; Stupak, J.; Jakubek, Z.; Whitfield, D. *J. Phys. Chem. C* **2009**, *113*, 3390–3401.

(17) Wang, R.; Ratcliffe, C. I.; Wu, X.; Voznyy, O.; Tao, Y.; Yu, K. *J. Phys. Chem. C* **2009**, *113*, 17979–17982.

(18) Yu, K.; Hu, M. Z.; Wang, R.; Piolet, M.; Frotey, M.; Zaman, Md. B.; Wu, X.; Leek, D. M.; Tao, Y.; Wilkinson, D.; Li, C. *J. Phys. Chem. C* **2010**, *114*, 3329–3339.

(19) Ouyang, J.; Schuurmans, C.; Zhang, Y.; Nagelkerke, R.; Wu, X.; Kingston, D.; Wang, Z. Y.; Wilkinson, D.; Li, C.; Leek, D. M.; Tao, Y.; Yu, K. *ACS Appl. Mater. Interfaces* **2011**, *3*, 553–565.

(20) Zhao, N.; Qi, L. *Adv. Mater.* **2006**, *18*, 359–362.

(21) Schliehe, C.; Juarez, B. H.; Pelletier, M.; Jander, S.; Greshnykh, D.; Nagel, M.; Meyer, A.; Foerster, S.; Kornowski, A.; Klinke, C.; Weller, H. *Science* **2010**, *329*, 550–553.

(22) Steckel, J. S.; Yen, B. K. H.; Oertel, D. C.; Bawendi, M. G. *J. Am. Chem. Soc.* **2006**, *128*, 13032–13033.

(23) Joo, J.; Pietryga, J. M.; McGuire, J. A.; Jeon, S.-H.; Williams, D. J.; Wang, H.-L.; Klimov, V. I. *J. Am. Chem. Soc.* **2009**, *131*, 10620–10628.

(24) Evans, C. M.; Evans, M. E.; Krauss, T. D. *J. Am. Chem. Soc.* **2010**, *132*, 10973–10975.

(25) Scherrer, P.; Göttingen, N. G. W. *Math.-Physik. Klasse* **1918**, 98.

(26) Nien, Y.-T.; Zaman, B.; Ouyang, J.; Chen, I.-G.; Hwang, C.-S.; Yu, K. *Mater. Lett.* **2008**, *62*, 4522–4524.

(27) Yu, W. W.; Falkner, J. C.; Shih, B. S.; Colvin, V. L. *Chem. Mater.* **2004**, *16*, 3318–3322.

(28) Wehrenberg, B. L.; Wang, C.; Guyot-Sionnest, P. *J. Phys. Chem. B* **2002**, *106*, 10634–10640.

■ NOTE ADDED AFTER ASAP PUBLICATION

This paper was published on the Web on April 8, 2011. Due to a production error, additional information was added to equation bM and the corrected version was reposted on April 13, 2011.